Supplementary information

Title

FIP200 is required for maintenance and differentiation of postnatal neural stem cells

Authors

Chenran Wang, Chun-Chi Liang, Z. Christine Bian, Yuan Zhu, and Jun-Lin Guan

Supplementary Figure 1 Analysis of the SVZ, DG and OB of *FIP200*^{hGFAP} cKO mice at different ages.

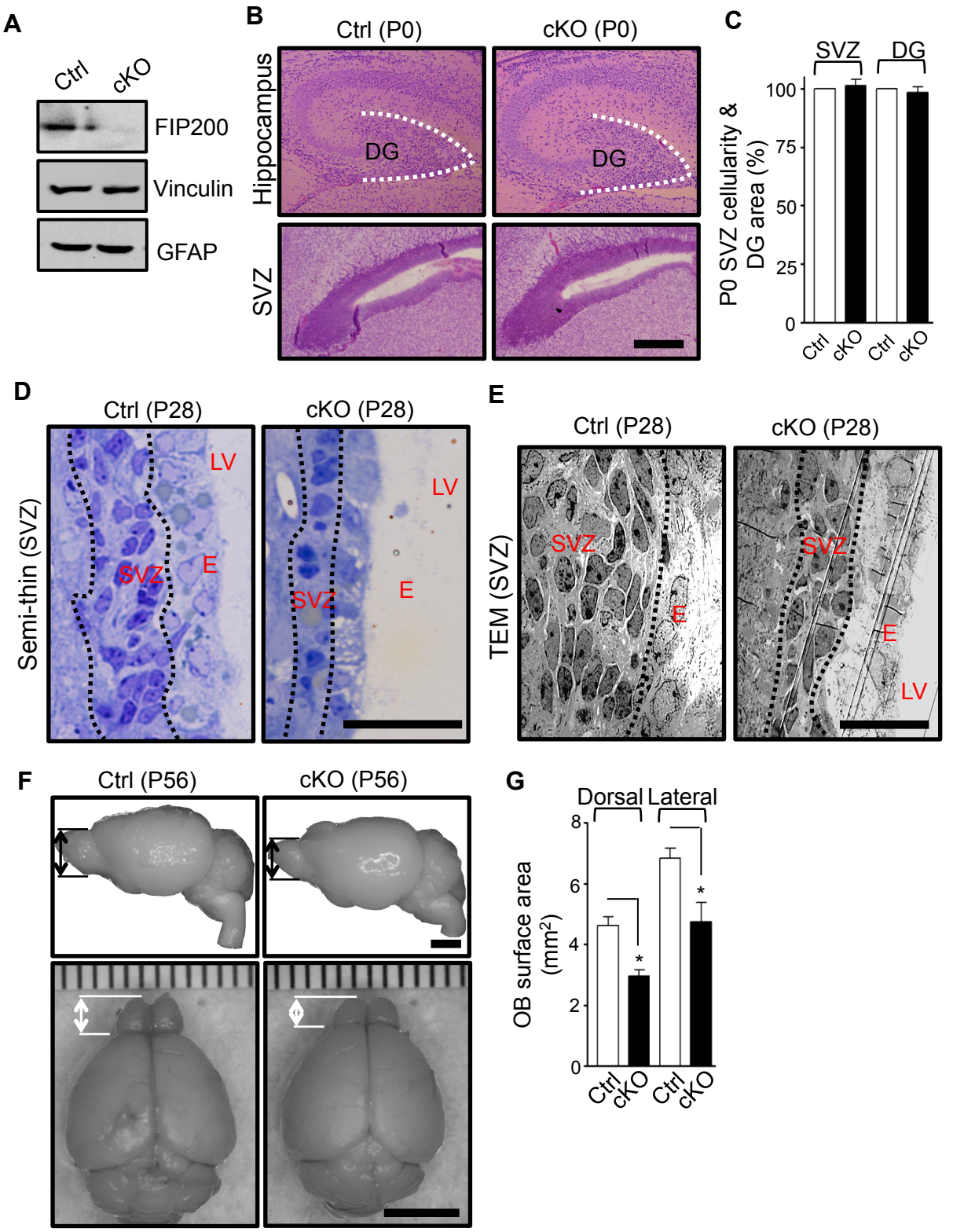

Supplementary Figure 1: (A) Lysates are extracted from the SVZ of Ctrl or *FIP200*^{hGFAP} cKO mice at P14 and analyzed by Western blot using anti-FIP200 (top), anti-Vinculin (middle) or anti-GFAP (bottom) antibodies. (B) H&E staining of hippocampus (upper panels) and the SVZ (lower panels) from Ctrl and *FIP200*^{hGFAP} cKO mice at P0. Lines indicate the boundaries of DG. Scale bars, 200 μm. (C) Mean±SE of the relative percentage of the SVZ cellularity and DG area per section are shown (n= 3 mice for each; ≥5 sections for each mouse). (D) Toluidine Blue O staining of semi-thin sections of the SVZ from Ctrl and *FIP200*^{hGFAP} cKO mice at P28. Lines indicate the boundaries of the SVZ. Scale bars, 40 μm. (E) TEM of the SVZ from Ctrl and *FIP200*^{hGFAP} cKO mice at P28. Lines indicate the boundaries of the SVZ. n= 2 mice for each. Scale bars, 20 μm. (F) Sagital (upper) and horizontal (lower) view of brains from Ctrl and *FIP200*^{hGFAP} cKO mice at P56. Scale bars, 5 mm. (G) Mean±SE of the OB surface area are shown (n= 3 mice for each). *: p<0.01.

Supplementary Figure 2 Analysis of NSC differentiation in *FIP200*^{hGFAP} cKO mice.

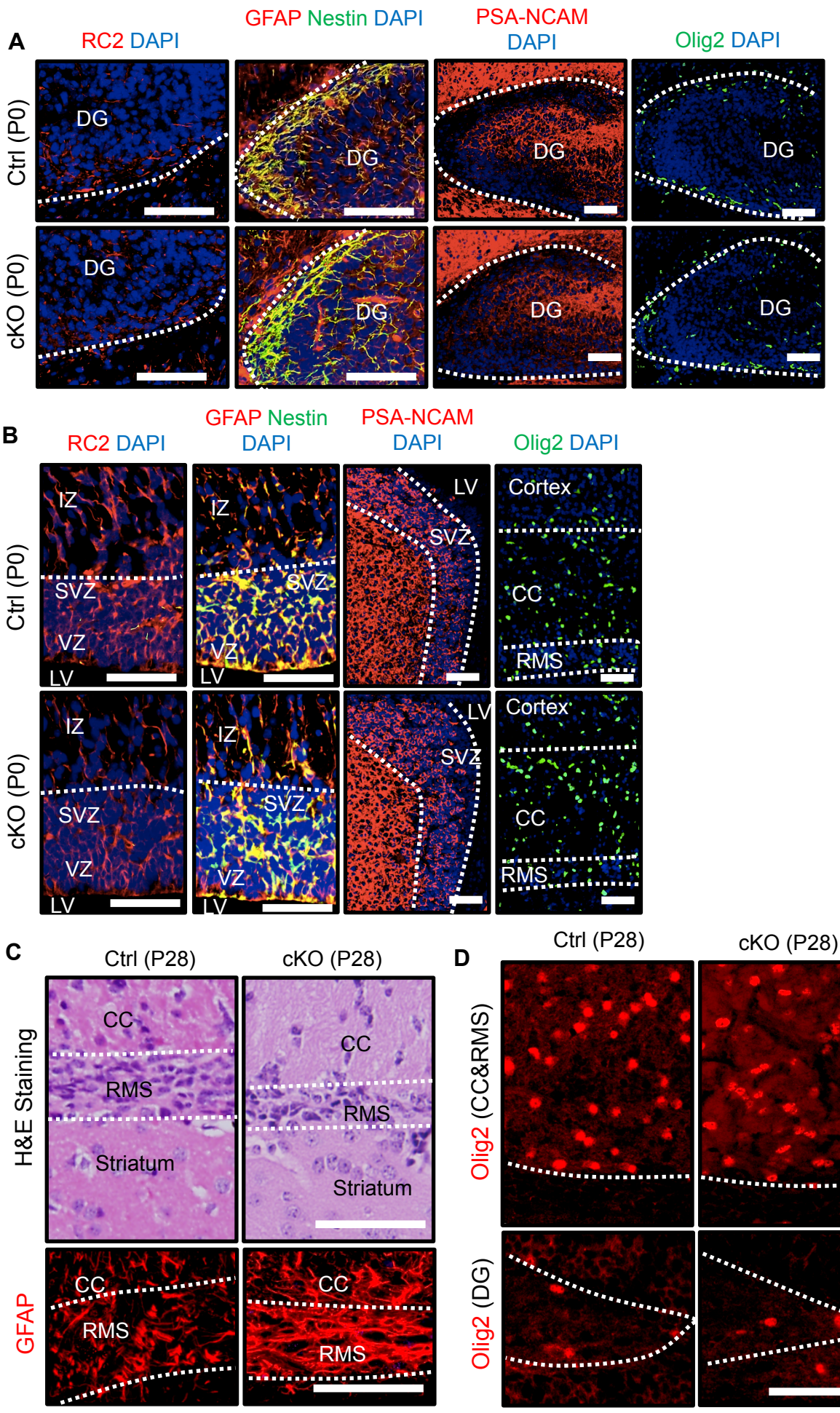

Supplementary Figure 2: Sections containing the DG (A), CC, cortex, VZ, SVZ, and RMS (B) of Ctrl and *FIP200*^{hGFAP} cKO mice at P0 are stained with various markers as indicated. Lines indicate the boundaries of the DG (A), VZ, SVZ, CC, and RMS (B). n= 3 mice for each. Scale bars, 50 μm. (C) Sections containing the RMS and adjacent regions of Ctrl and *FIP200*^{hGFAP} cKO mice at P28 are examined by H&E staining (top) or immunofluorescent staining with GFAP (bottom). Lines indicate the boundaries of the RMS. n= 3 mice for each. Scale bars, 50 μm. (D) Sections containing the CC, RMS (top) or DG (bottom) of Ctrl and *FIP200*^{hGFAP} cKO mice at P28 are examined by immunofluorescent staining with Olig2. Lines indicate the boundaries of the CC (top) and DG (bottom). n= 3 mice for each. Scale bars, 50 μm.

Supplementary Figure 3 Analysis of apoptosis in newborn *FIP200*^{hGFAP}cKO mice.

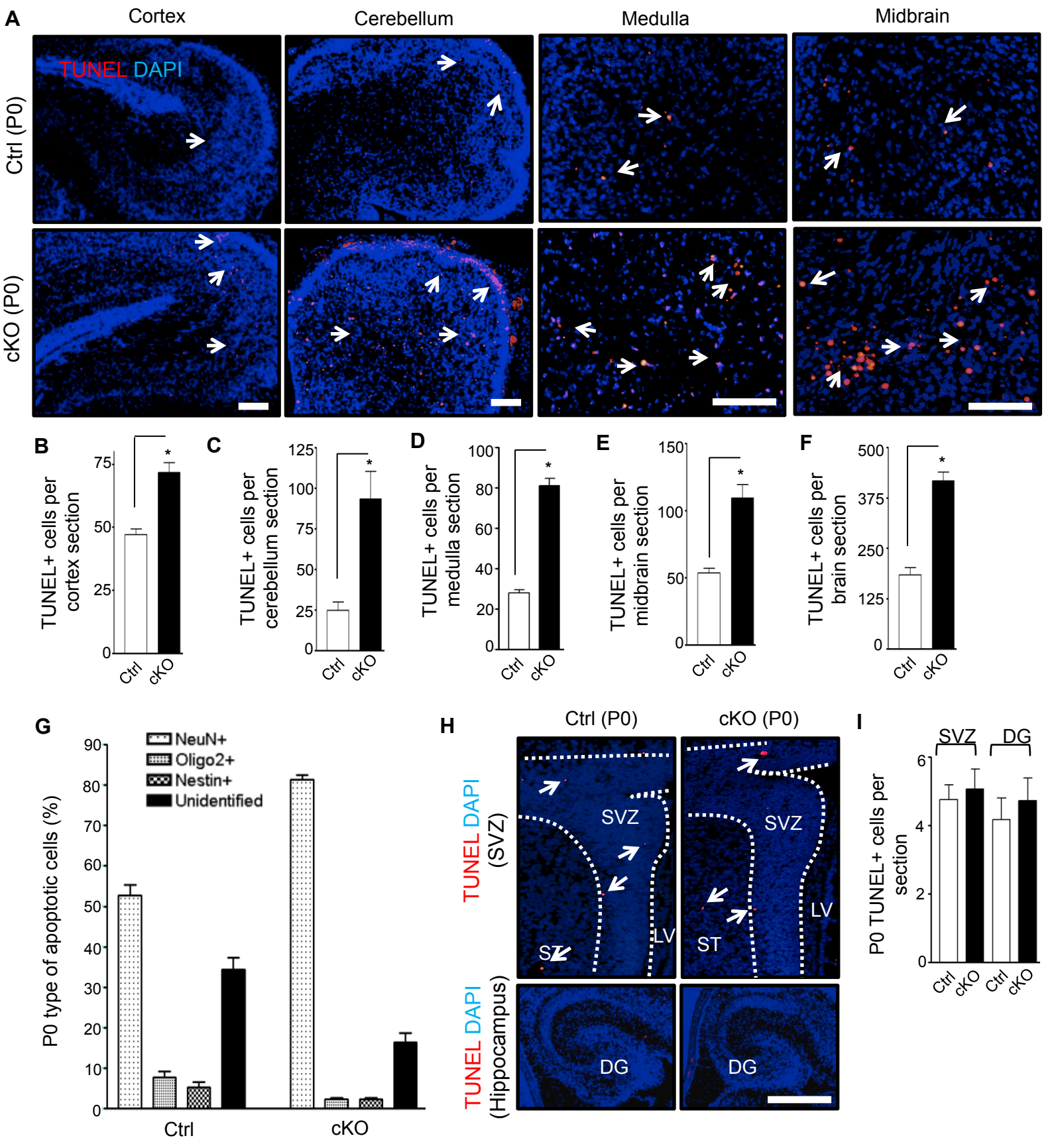

Supplementary Figure 3: (A) TUNEL and DAPI staining of the cortex, cerebellum, medulla, and midbrain from Ctrl and *FIP200*^{hGFAP} cKO mice at P0. Arrows mark TUNEL$^+$ cells. Scale bars, 50 μm. (B-F) Mean±SE of TUNEL$^+$ cell numbers per section of different brain regions are shown (n= 3 mice for each, ≥4 sections for each mouse). (G) Whole brain sections from Ctrl or *FIP200*^{hGFAP}cKO mice at P0 are subjected to TUNEL assays along with staining for various markers. Mean±SE of the percentages of NeuN$^+$/TUNEL$^+$, Olig2$^+$/TUNEL$^+$, and Nestin$^+$/TUNEL$^+$ cells are shown (n= 3 mice for each, ≥4 sections for each mouse). Unidentified percentage represents cells negative for all 3 markers. (H) TUNEL and DAPI staining of the SVZ and hippocampus from Ctrl and *FIP200*^{hGFAP} cKO mice at P0. Lines indicate the boundaries of the SVZ. Arrows mark TUNEL$^+$ cells. (I) Mean±SE of TUNEL$^+$ cell numbers per section containing the SVZ and hippocampus are shown (n= 3 mice for each; ≥4 sections for each mouse). Scale bars, 50 μm. *: p<0.01.

Supplementary Figure 4 Analysis of cell proliferation in the SVZ and DG of *FIP200*^{hGFAP} cKO mice.

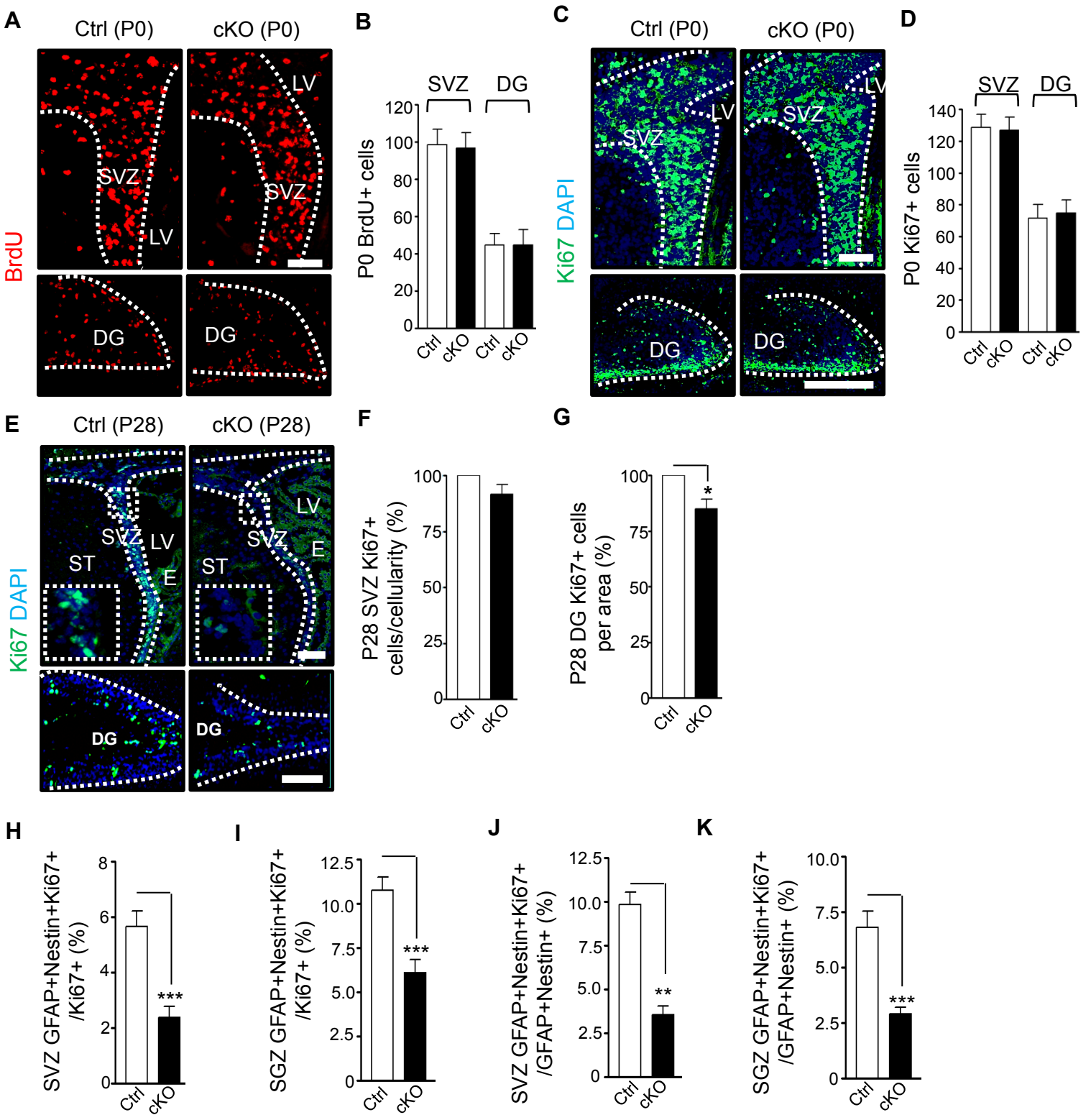

Supplementary Figure 4: (A-D) Short-term BrdU incorporation (A, B) and Ki67, DAPI staining (C, D) in the SVZ and DG of Ctrl and *FIP200*^{hGFAP}cKO mice at P0. Representative images are shown in A and C. Lines indicate the boundaries of the SVZ and DG. Mean±SE of BrdU$^+$ (B) and Ki67$^+$ (D) cell numbers per section in the SVZ and DG are shown (n= 3 mice for each; ≥4 sections for each mouse). Scale bars, 50 μm. (E) Ki67 and DAPI staining in the SVZ and DG of Ctrl and *FIP200*^{hGFAP}cKO mice at P28. Lines indicate the boundaries of the SVZ and DG. The boxed areas in E are shown in more detail for staining of Ki67 and DAPI in the SVZ in insets. Mean±SE of the relative percentage of Ki67$^+$ cells (standardized to Ctrl mice as 100%) normalized with the SVZ cellularity (F) and DG area (G) are shown (n= 3 mice for each; >500 Ki67$^+$ cells from ≥4 sections counted from each mouse). Scale bars, 50 μm. (H, I) Mean±SE of the percentage of GFAP$^+$/Nestin$^+$/Ki67$^+$ cells normalized to total Ki67$^+$ cells in the SVZ (H) and SGZ (I) of Ctrl and *FIP200*^{hGFAP}cKO mice are shown (n= 5 mice each, >300 Ki67$^+$ cells for SVZ and ≥4 sections for DG of each mouse). (J, K) Mean±SE of the percentage of GFAP$^+$/Nestin$^+$/Ki67$^+$ cells normalized to total GFAP$^+$/Nestin$^+$ NSCs in the SVZ (J) and SGZ (K) of Ctrl and *FIP200*^{hGFAP}cKO mice are shown (n= 5 mice each, >200 GFAP$^+$/Nestin$^+$ cells for SVZ and ≥4 sections for DG of each mouse). *: p<0.05, **: p<0.01, ***: p<0.001.

Supplementary Figure 5 Inactivation of *p53* could not rescue the neurogenesis defects in the OB and autophagy defects in the SVZ of *FIP200*^{hGFAP} cKO mice.

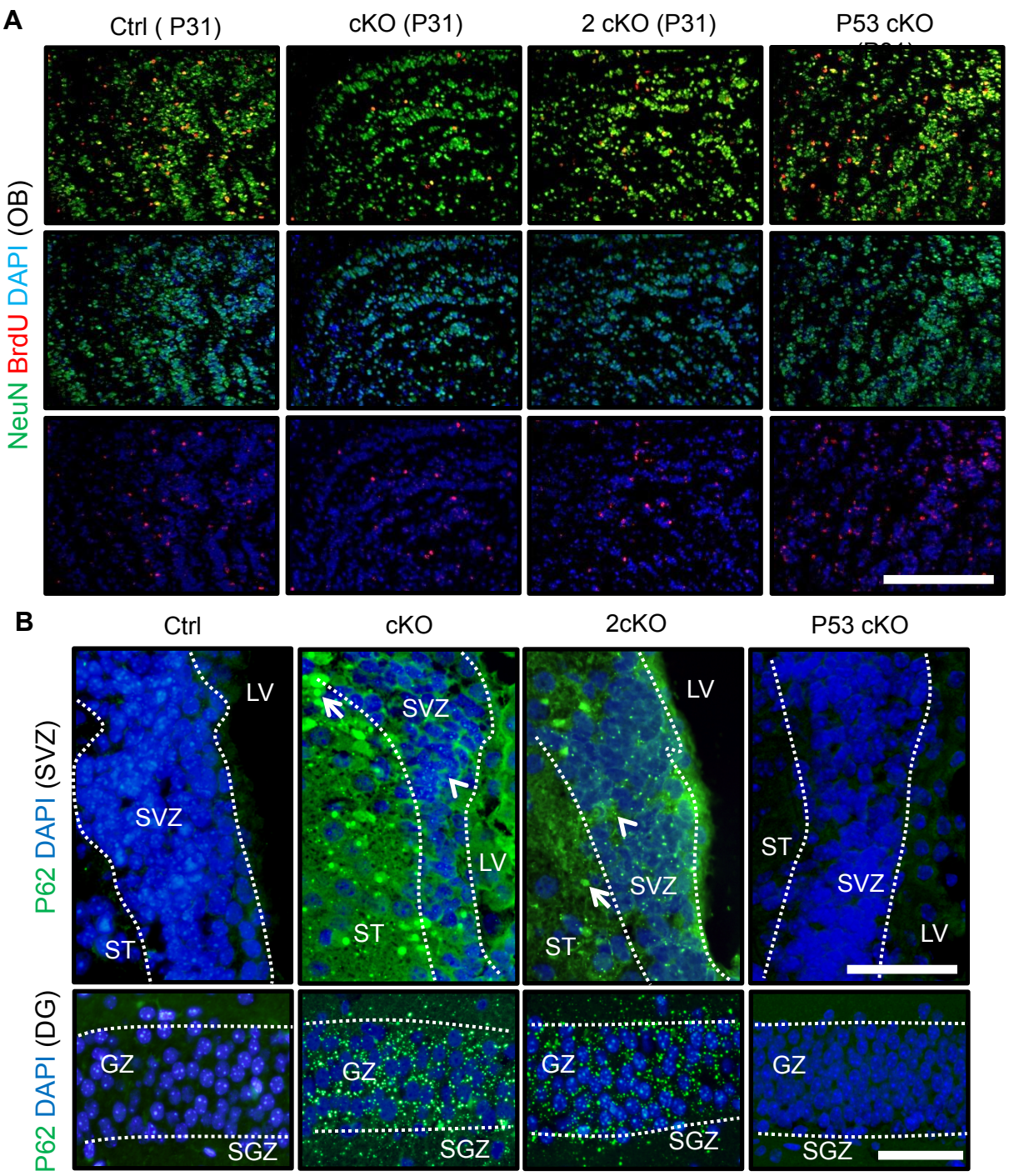

Supplementary Figure 5: (A) Immunofluorescent staining of NeuN and DAPI with long-term incorporated BrdU in the OB from Ctrl, *FIP200*^{hGFAP} cKO, 2cKO, and *p53*^{hGFAP} cKO mice at P31. The middle and bottom panels are shown for staining of NeuN/DAPI and BrdU/DAPI separately. n= 5 mice for each. Scale bars, 100 μm. (B) Immunofluorescence of p62 and DAPI in the SVZ and DG of Ctrl, *FIP200*^{hGFAP} cKO, 2cKO, and *p53*^{hGFAP} cKO mice at P28. Lines indicate the boundaries of GZ and SVZ. The arrows and arrowheads mark larger and smaller p62^{+} aggregates in the ST and SVZ, respectively. n= 3 mice for each. Scale bars, 30 μm.

Supplementary Figure 6 NAC treatment rescues the aberrant increase of *p53* and its target genes, neurosphere formation defects, and the neurogenesis defects in *FIP200*^{hGFAP} cKO mice.

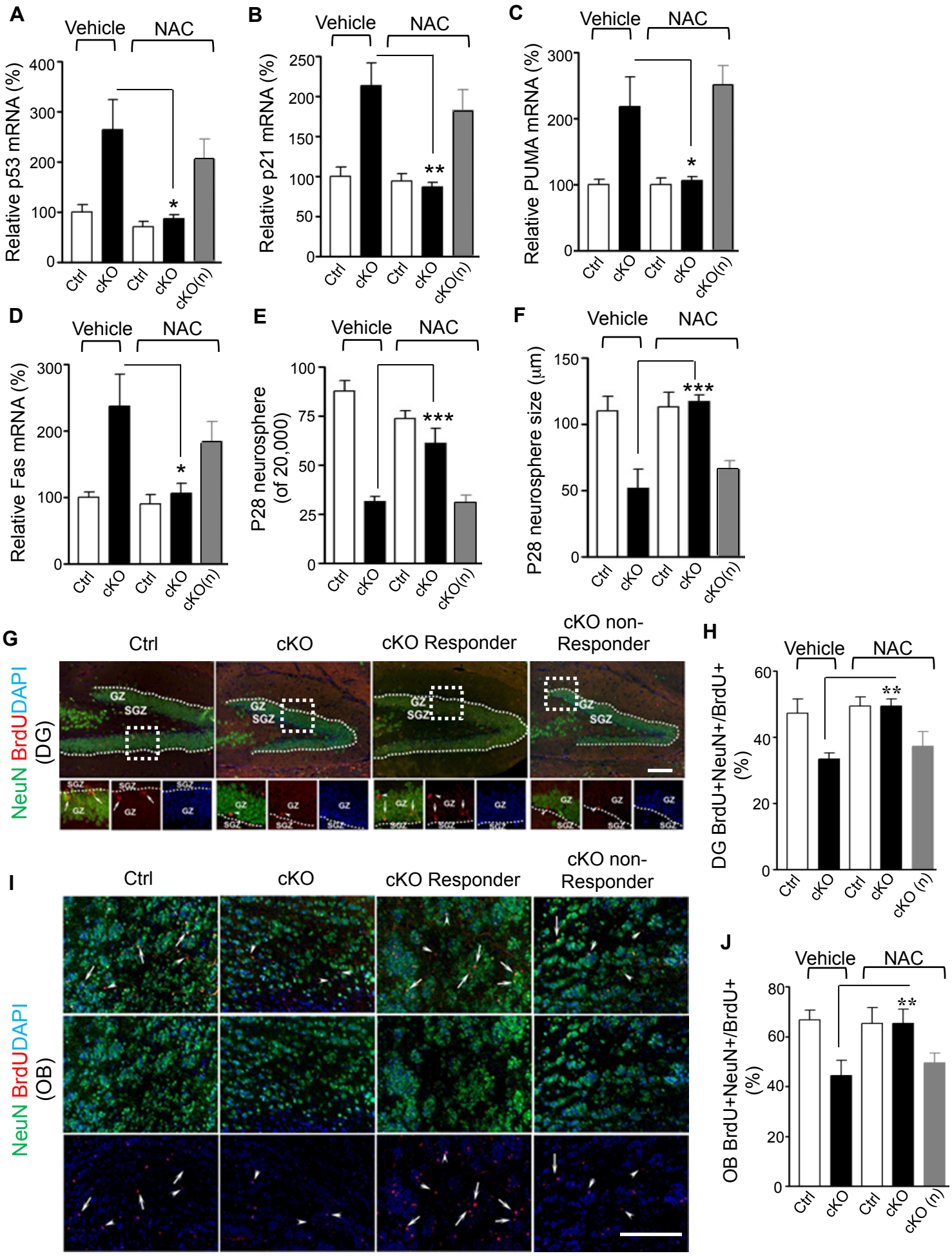

Supplementary Figure 6: (A-D) Mean±SE of relative mRNA level (normalized to vehicle treated Ctrl mice as 100%) of *p53*, *p21*, *PUMA*, and *Fas* in neurospheres from Ctrl and *FIP200*^{hGFAP} mice treated with or without NAC are shown (n= 4 mice for each). (E, F) Mean±SE of the number (E) and size (F) of primary neurospheres of Ctrl and *FIP200*^{hGFAP} cKO mice at P28 treated with or without NAC are shown (n= 4 mice for each). (G-J) Immunofluorescence of long-term retained BrdU, NeuN and DAPI in the DG (G, H) and OB (I, J) from Ctrl, *FIP200*^{hGFAP} cKO mice treated with vehicle or NAC at P28. The boxed areas in upper panels of (G) are shown in more detail for staining in lower panels. Lines indicate the boundaries of DG in the upper panels and boundaries between GZ and SGZ in the lower panels. The middle and bottom panels of (I) are shown for staining of NeuN/DAPI and BrdU/DAPI separately. Arrows mark NeuN$^+$/BrdU$^+$ cells and arrowheads mark NeuN$^-$/BrdU$^+$ cells in the DG (G) and OB (I). Mean±SE of the percentage of NeuN$^+$/BrdU$^+$ cells of total long term BrdU retained cells in the DG (H) and OB (J) are shown (n= 5 mice for each; >20 BrdU$^+$ cells counted for DG). cKO(n): NAC non-responder *FIP200*^{hGFAP} cKO mice. Scale bars, 100 μm. *: p<0.05; **: p<0.01, ***: p<0.001.

Supplementary Figure 7 Expression of Notch and its targets in neurospheres are not changed in *FIP200*^{hGFAP} cKO mice.

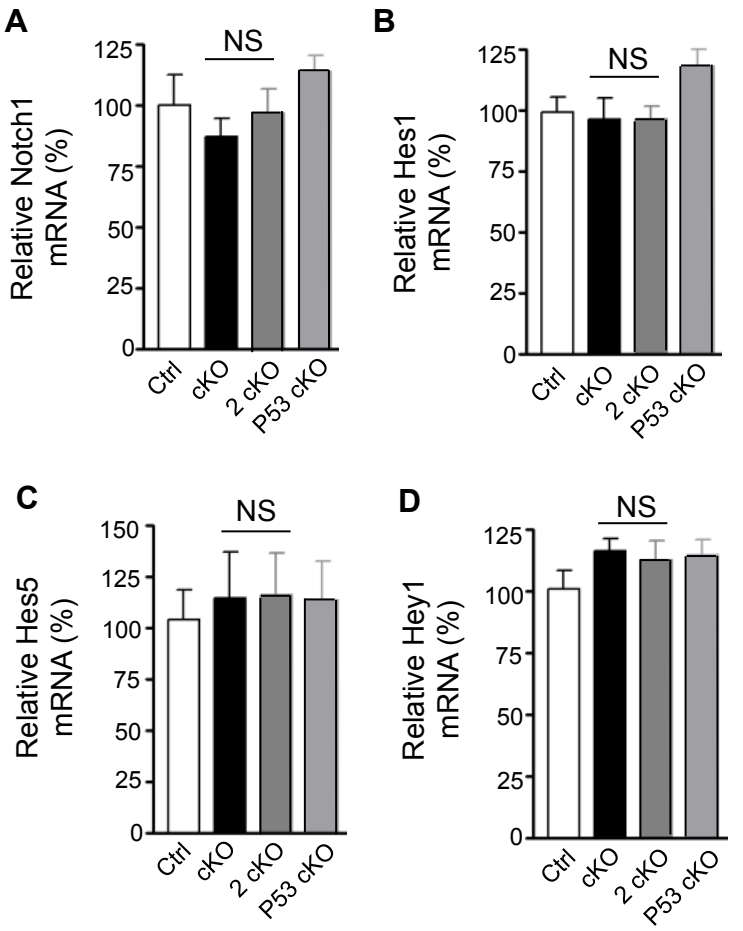

Supplementary Figure 7: (A-D) Mean±SE of relative mRNA level (normalized to Ctrl mice as 100%) of Notch1 (A), Hes1 (B), Hes5 (C), and Hey1 (D) in neurospheres of Ctrl, *FIP200*^{hGFAP} cKO, 2cKO, and *p53*^{hGFAP} cKO mice are shown (n= 3 mice for each). NS: no significance.

Supplementary Figure 8 NAC treatment rescues the abnormal genes expression and neurosphere formation defects in *FIP200*^{hGFAP} cKO mice.

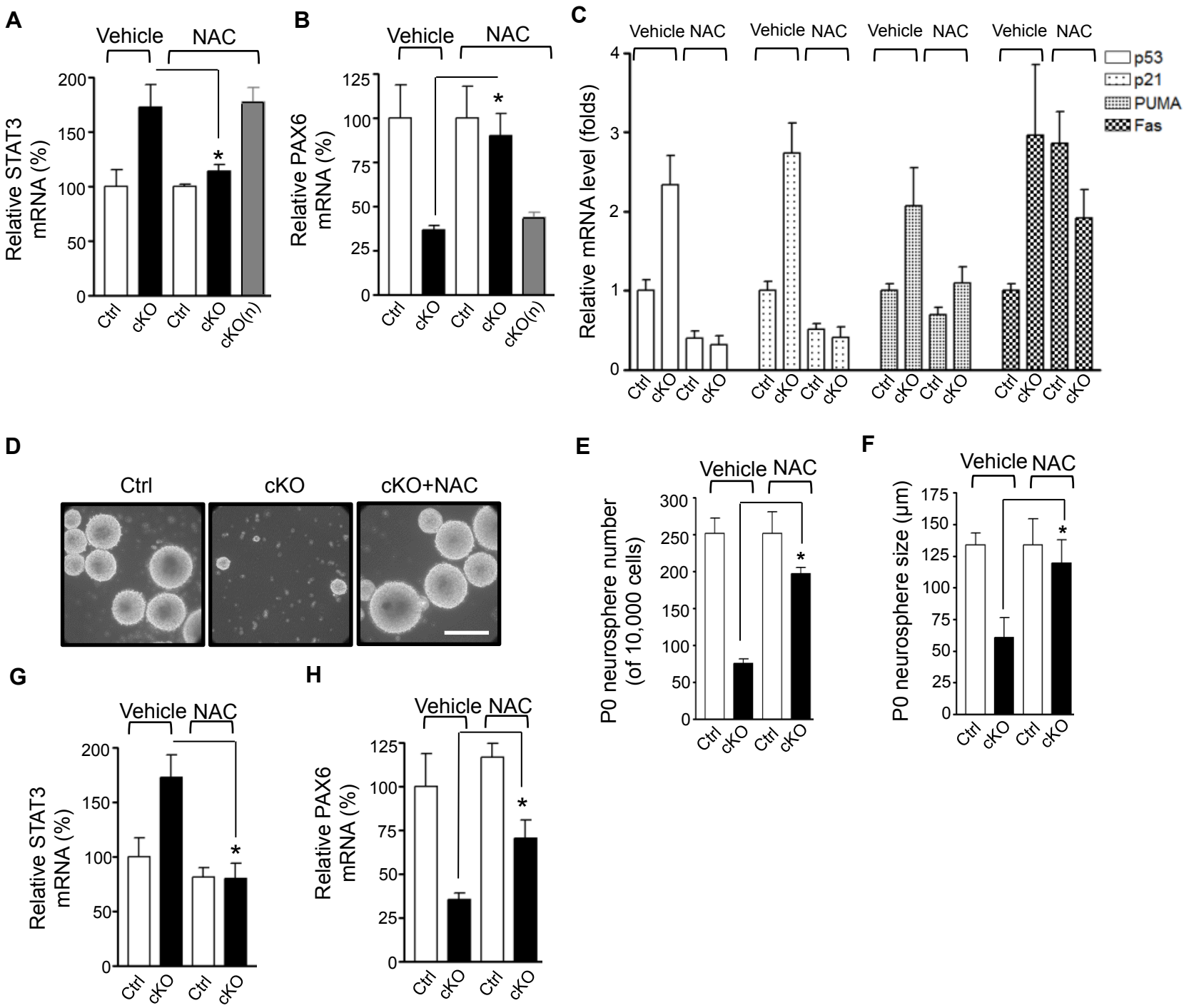

Supplementary Figure 8: (A, B) Mean±SE of relative mRNA level (normalized to vehicle treated Ctrl mice as 100%) of *STAT3* (A) and *PAX6* (B) in neurospheres from Ctrl and *FIP200*^{hGFAP} mice treated with or without NAC are shown (n= 4 mice for each). cKO(n): NAC non-responder *FIP200*^{hGFAP} cKO mice. (C) Mean±SE of relative mRNA level (normalized to vehicle treated Ctrl neurosphere as 1) of *p53*, *p21*, *PUMA*, and *Fas* of Ctrl and *FIP200*^{hGFAP} cKO neurospheres treated with vehicle or NAC for 10 days are shown (n= 3 mice for each). (D) Phase contrast images of secondary neurospheres from Ctrl and *FIP200*^{hGFAP} cKO mice at P0 cultured in the presence or absence of NAC. Scale bars, 75 μm. Mean±SE of the number (E) and size of neurospheres (F) are shown (n= 3 mice for each). (G, H) Mean±SE of relative mRNA level (normalized to vehicle treated Ctrl neurosphere as 100%) of *STAT3* (G) and *PAX6* (H) of Ctrl and *FIP200*^{hGFAP} cKO neurospheres treated with vehicle or NAC are shown (n= 3 mice for each). *: $p<0.05$.

Supplementary Figure 9 Effects of Spautin-1 and co-culture with astrocytes on neurosphere formation and analysis of autophagy activity in embroynic and postnatal NSCs.

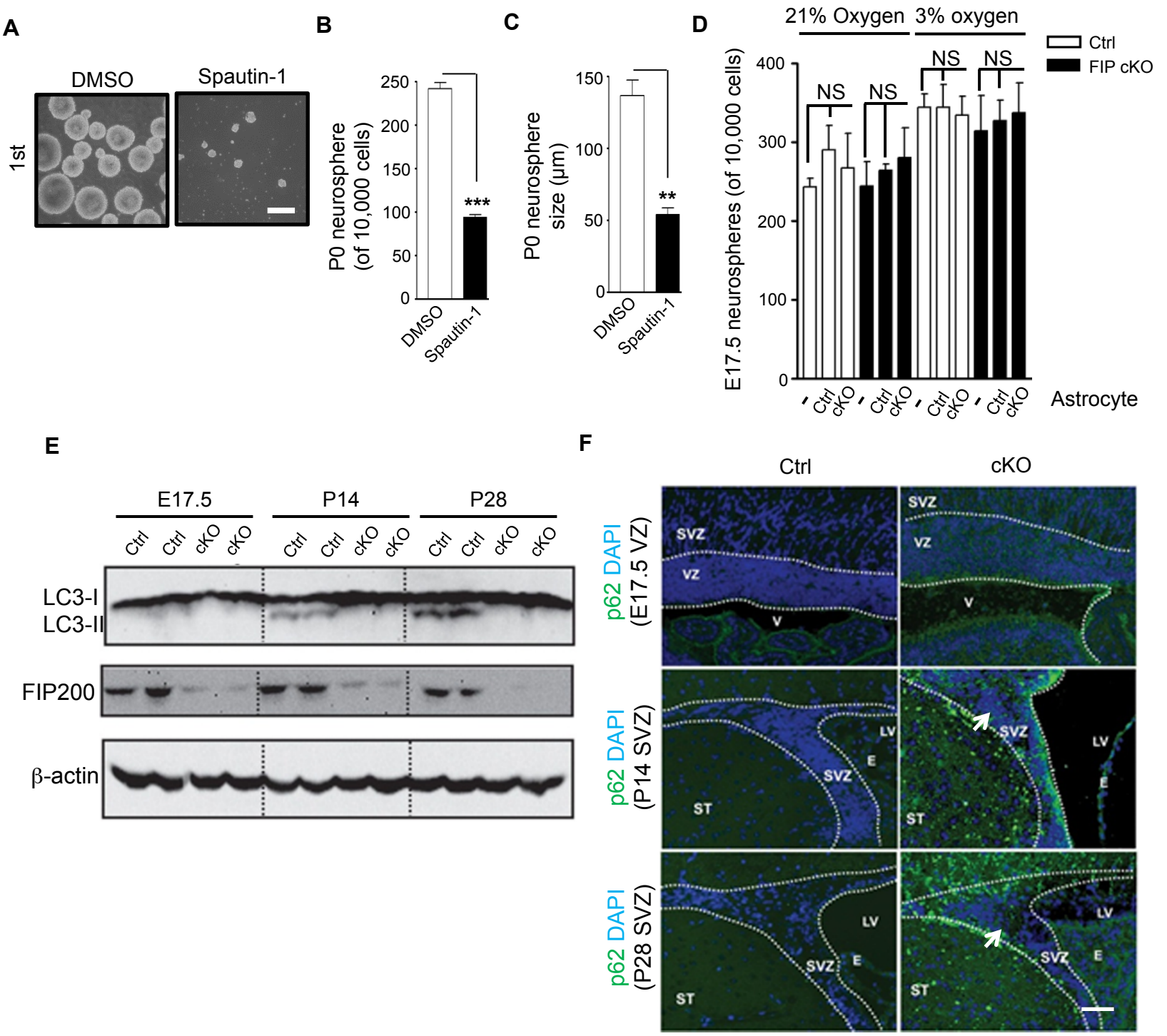

Supplementary Figure 9: (A) Primary neurospheres from Ctrl mice at P0 were treated with DMSO or 10 μM Spautin-1. Representative phase contrast images are shown in (A). Scale bars, 100 μm. Mean±SE of number (B) and size (C) of neurospheres are shown (n= 3 mice for each). (D) Embryonic NSCs from Ctrl and *FIP200*^{hGFAP} cKO mice at E17.5 are cultured alone or co-cultured with postnatal astrocytes from ctrl and *FIP200*^{hGFAP} cKO mice for 10 days. Mean±SE of the number of primary neurospheres cultured under 3% and 21% oxygen conditions are shown (n= 3 mice for each). (E) Lysates were extracted from the cortex (E17.5) and SVZ (P14 and P28) of 2 different Ctrl and *FIP200*^{hGFAP} cKO mice and analyzed by Western blot using anti-LC3 (top), anti-FIP200 (middle), and anti-beta-actin (bottom) antibodies, as indicated. (F) Immunofluorescence of p62 and DAPI in the VZ and SVZ of Ctrl and *FIP200*^{hGFAP} cKO mice at E17.5, P14 and P28. Lines indicate the boundaries of the VZ and SVZ. Arrows indicated SVZ of *FIP200*^{hGFAP} cKO mice at P14 and P28. n= 3 mice for each. Scale bar, 50 μm. NS: no significance; **: $p<0.01$; ***: $p<0.001$.

Supplementary Figure 10 Analysis of ROS levels in embryonic VZ and postnatal SVZ.

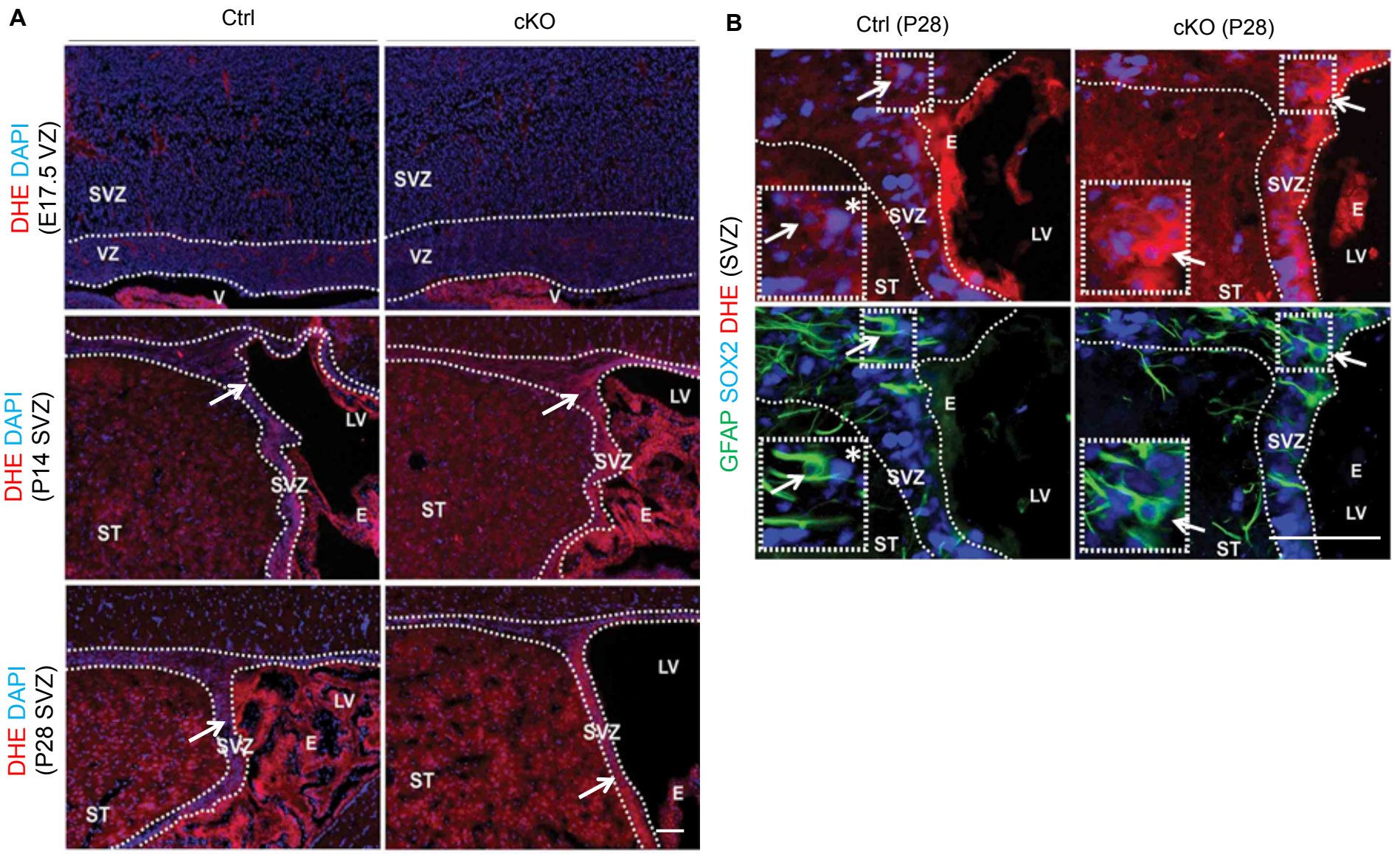

Supplementary Figure 10: (A) Immunofluorescence of DHE and DAPI in the VZ and SVZ of Ctrl and *FIP200*^{hGFAP} cKO mice at E17.5, P14 and P28, as indicated. Lines indicate the boundaries of the VZ and SVZ. Arrows indicated SVZ. n= 3 mice for each. Scale bar, 50 μm. (B) Immunofluorescence of GFAP, SOX2, and DHE in the SVZ from Ctrl and *FIP200*^{hGFAP} cKO mice at P28. Lines indicate the boundaries of the SVZ. The boxed areas are shown in more detail for staining of GFAP, SOX2 and DHE. Arrows mark GFAP^{+}/SOX2^{+} cells with DHE signal at different levels and asterisks mark a GFAP^{+}/SOX2^{+} cell in Ctrl SVZ without DHE signal. Scale bar, 50 μm.

Supplementary Figure 11 Full-length pictures of the blots presented in the main figures.

Figure 1 A

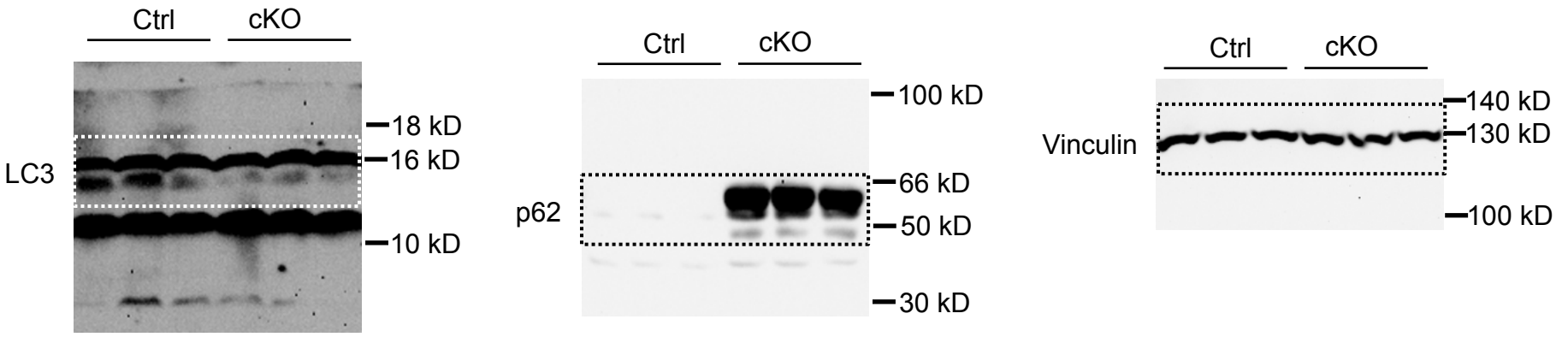

Figure 4 A